Effect of Carbon Nanotube-Supported β Nucleating Agent on the Thermal Properties, Morphology, and Mechanical Properties of Polyamide 6/Isotactic Polypropylene Blends

Jie Li, Shi-Wei Wang, Ke-Jun Zhan, Wei Yang, Bang-Hu Xie, Ming-Bo Yang

College of Polymer Science and Engineering, Sichuan University, State Key Laboratory of Polymer Materials Engineering, Chengdu 610065, Sichuan, People's Republic of China

Received 30 November 2010; accepted 22 June 2011
DOI 10.1002/app.35137
Published online 11 October 2011 in Wiley Online Library (wileyonlinelibrary.com).

ABSTRACT: A new kind of β nucleating agent, multi-wall carbon nanotube (MWCNT)-supported calcium pimelate was introduced into polyamide 6 (PA 6)/isotactic polypropylene (iPP; 10/90 by weight) blend and the thermal properties, morphology, and mechanical properties were investigated. The results showed that β-iPP appeared at low content of MWCNT-supported calcium pimelate which surmounted the α-nucleating effect of PA 6 for iPP, and the content of β-iPP increased with increasing content of MWCNT-supported calcium pimelate. The impact strength, elongation at break, and flexural modulus were improved with increasing content of MWCNT-supported calcium pimelate without significantly deteriorating the tensile strength. J Appl Polym Sci 124: 993–999, 2012

Key words: polyamide 6/isotactic polypropylene blends; β nucleating agent; calcium pimelate; multi-wall carbon nanotube

INTRODUCTION

Isotactic polypropylene (iPP), one of the most popular thermoplastic polymers with good mechanical properties, chemical stability, low cost, and easy-processing characteristic, is a semicrystalline polymer with three main crystal modifications including monoclinic (α), trigonal (β), and orthorhombic (γ).[1,2] The β form iPP has been widely studied due to its high deformation temperature (HDT) and excellent impact strength.[3] While α crystals with greater stability than crystals of other modifications develop under practical processing conditions easily, the occurrence of metastable β form can be obtained by (1) directional crystallization in a temperature gradient field[4]; (2) shear- or elongation-induced crystallization[5] and (3) the introduction of specific nucleating agent, i.e., β nucleating agent (β-NA), which is the most effective and accessible method to obtain iPP with high content of β crystals.[6–10]

Until now, at least four classes of compounds may be used as β-NAs: condensed-ring compounds with quasi-planar structure, such as γ-modification of linear *trans*-quinacridone (γ-TLQ) which is a commercial red pigment (Permanentrot E3B)[11]; Ca salts of different dicarboxylic acids[2,8,12]; aryl amide derivatives (TMB-5);[13–16] and rare earth nucleating agents (WBG).[17,18] Recently, Phillips et al.[19] found that semicrystalline isotactic polystyrene (iPS) can also be used as a selective β-NA for iPP in the quiescent condition and during isothermal crystallization the shear-induced nuclei promoted an orientation form of crystal growth and accelerated the crystallization kinetics. It is generally accepted that with the introduction of β-NAs, impact strength and heat distortion temperature of iPP are improved at the expense of stiffness of iPP.[20]

For decades, polymer blends have received great attention owning to the combination of properties from the components. PA 6/iPP blends, which have been extensively studied owing to the good combination of mechanical properties from PA 6 and the inertness to humidity and ease of processing from iPP. However, PA 6 and iPP are thermodynamically immiscible and the resultant PA 6/iPP blends usually exhibit heterogeneous phase morphology and inferior mechanical performance. Therefore, compatibilizers, usually copolymers[7,21–24] are widely used to reduce the surface tension and to improve interfacial adhesion. Agrawal[21] used polypropylene grafted with acrylic acid (PP*g*AA) or with maleic anhydride (PP*g*MA) as the compatibilizers and the impact strength of the blends containing PP*g*MA were much higher than those of the blends containing PP*g*AA due to a considerable improvement of

Correspondence to: W. Yang (ysjsanjin@163.com).
Contract grant sponsor: National Natural Science Foundation of China; contract grant numbers: 50973074, 51073110.
Contract grant sponsor: Fok Ying Tung Education Foundation; contract grant number: 122022.

interfacial adhesion between PA 6 and PP components. Macro et al.[25] adopted PP*g*MA to compatibilize PA 6/iPP blends and found that the presence of PP*g*MA leads to a reduction in the crystallinity and rate of crystallization of PA 6 because of the diluent effect of the molten iPP. Apart from compatilizer, organic fillers were widely introduced into PA 6/PP blends to ameliorate the comprehensive properties. Kusomono et al.[24] introduced four different types of organophilic montmorillnite (OMMT) and SEBS-*g*-MA into PA6/PP blends, and found that both OMMT and SEBS-*g*-MA could balance properties between strength, stiffness, and toughness. Othman et al.[26] adopted a maleated polyethylene-octene elastomer (POE*g*MAH) to modify PA 6/PP/organophilic modified montmorillonite (MMT) nanocomposites, and the Young's modulus and flexural modulus were improved with increasing MMT concentration at the expense of toughness and ductile properties.

Aiming at improving the toughness of PA 6/PP blend, some works have been done to produce PA 6/iPP blends with high content of β-iPP. Different from the case that amorphous polymers have little influence on the formation of β-iPP[25,27] of iPP-based blends, for iPP-based blends with other semicrystalline polymers, especially those with α nucleating ability for iPP, such as poly(vinylidene fluoride) and polyamide,[10,17] the condition is much more complicated. If the crystallization temperature (T_c) of the second component is higher than that of iPP, it will intensely suppress the formation of β-iPP; oppositely, lower T_c of the second component has little effect on the formation of β-iPP. Yang et al.[28,29] confirmed that compounding conditions and compatibilizer type also profoundly influences the content of β-iPP in β-nucleated PA 6/iPP blends.

It should be noticed that the toughness of β-iPP is improved at the expense of stiffness. Nowadays, multi-wall carbon nanotubes (MWCNTs) were widely adopted in polymers or polymer blends due to their unique physical and mechanical characteristics, such as high Young's modulus and strength.[30–32] Zhang et al.[32] showed that carbon nanotubes can act as heterogeneous nucleating agents for PP transcrystallization and the nucleation of PP first occurs at the surface of nanotubes and grows into transcrystals perpendicular to the nanotude axis. Via solvent and "solvent-free" dry mixing method for dispersing MWCNTs in PP, enhancements in yield strength, hardness and Young's modulus can be achieved.[30]

In our previous work, calcium pimelate, a kind of highly selective β-NA, was chemically supported onto MWCNTs[31] and then was introduced into iPP. The results exhibited an enhanced nucleating ability of the MWCNTs-supported β-NA, and the impact toughness of the iPP-based composites was significantly improved without deteriorating the strength and stiffness greatly. In this work, the calcium pimelate was chemically supported onto the surface of MWCNTs and the resultant MWCNTs-supported β-NA was introduced into PA 6/iPP blends to reveal the effect of this novel β nucleating agent for PP on the melting, crystallization, morphology, and mechanical properties of PA 6/iPP blends.

EXPERIMENTAL

Materials

Commercial grade iPP (trademark T30S), with a melt flow rate (MFR) of 2.6 g/10 min (ASTM D-1238, 230°C, 2.16-kg load) and the isotactic index of 98%, was purchased from Lanzhou Petroleum Chemical, China. PA 6 (trademark M2800), commercially available, with a MFR of 11.0 g/10 min (ASTM D-1238, 230°C, 2.16-kg load) and a density of 1.14 g cm^{-3} was supplied by Guangdong Xinhui Meida Nylon, China. The MWCNTs with a diameter of about 8 nm and the length of 10–30 μm, synthesized from methane by means of catalytically chemical vapor deposition, was purchased from Chengdu Institute of Organic Chemistry, Chinese Academy of Science. The received MWCNTs were chemically treated with 3.7 wt % hydroxyl groups attaching to the tube walls.

Sample preparation

According to Varga[2] and Li and Cheung,[33] calcium pimelate was prepared with pimelic acid and calcium stearate of the same molar ratio, which assured that the calcium stearate can only react with one of the carboxyl groups of pimelic acid. Then, the prepared calcium pimelate and MWCNTs were dispersed in ethanol using a VCF-1500 ultrasonic irradiation instrument (Sonic and Materials, USA). Afterwards, the suspension was kept at 80°C for 1 h with a stirring rate of 1,000 r min^{-1} to chemically support calcium pimelate onto the surface of MWCNTs. Finally, the MWCNT-supported calcium pimelate was filtered, washed by ethanol, and dried into powder.

A two-step blending process was adopted to prepare the PA 6/iPP blends nucleated by the MWCNTs-supported calcium pimelate. First, a master batch of iPP with 5 wt % MWCNTs-supported calcium pimelate was produced within an internal mixer (XSS-300). Then, via an SHJ-20 corotating twin-screw extruder with a screw diameter of 25 mm, a length/diameter ratio of 32, and a temperature profile of 195–230°C from the feeding zone to the die, the master batch was melt blended with iPP and PA 6 at a weight proportion of PA 6/iPP of 10/

90 to obtain desired content of MWCNTs-supported calcium pimelate in the blends. Then the extrudate was quenched into water and pelletized. After drying to remove the moisture for 12 h under vacuum at 80°C, the pellets were injection-molded into dumb-bell tensile samples and standard rectangular impact samples on a PS40E5ASE precise injection-molding machine, with a temperature profile of 220–255°C from the feeding zone to the nozzle. The nucleated blend was named as P1-0.05 for example, with the decimal part representing the weight percentage of MWCNTs-supported calcium pimelate in the blend. For comparison, 0.05 wt % of calcium pimelate and 0.05 wt % of MWCNTs were introduced into the PA 6/iPP blend with the same processing procedure, respectively. These two samples were named as PNA-0.05 and PCNT-0.05, respectively.

Tests and characterization

The samples for DSC tests were taken from the core layer of the injection molded bars. DSC scanning of the samples was performed on a TA DSC Q20 differential scanning calorimeter in a nitrogen atmosphere. The calibration of the temperature and heat flow scales was performed with standard indium. Samples were heated quickly to 240°C and held at 240°C for 5 min to eliminate any thermal history, and then cooled to 100°C at a rate of 10°C min^{-1} to determine the crystallization behavior, after which they were heated again from 100 to 240°C at a rate of 10°C min^{-1}, and the melting behaviors were recorded. Thermograms were evaluated by means of Universal V2.6D (TA Instruments) software.

For XRD characterization, all the samples of injection molded bars, 1-mm away from the surface layer, were cut by an ultrathin semiautomatic microtome (KD-3358). Patterns of the specimens were recorded at ambient temperature (about 23°C) with a philips X'Pert Pro MPD DY1291 apparatus, equipped with Ni-filtered Cu Kα radiation with a wavelength of 0.154 nm, in the reflection mode. The operating condition of the X-ray source was set at a voltage of 40 kV and a current of 35 mA in a range of $2\theta = 12–30°$ with a step scanning rate of 2° min^{-1}. The β-iPP fraction (K_β) was calculated from XRD diffractogram according to the Turner-Jones formula[34]:

$$K_\beta = H^\beta_{300} / \left(H^\alpha_{110} + H^\alpha_{040} + H^\alpha_{130} + H^\beta_{300} \right) \qquad (1)$$

where H^α_{110}, H^α_{040}, and H^α_{130} are the intensities of, (110), (040), and (130) reflections of α-iPP, respectively, and H^β_{300} is the intensity of (300) reflection of β-iPP.

For morphology observation, injection-molded specimens were first cryogenically fractured in liquid nitrogen. The fracture surfaces were etched by formic acid to remove PA 6 phase, and then a mixed acid solution, containing 33 wt % concentrated sulfuric acid (H_2SO_4), 66 wt % concentrated phosphoric acid (H_3PO_4) and 1.3 wt % potassium permanganate ($KMnO_4$)[35] was used to etch the amorphous region of iPP on the fracture surface at ambient temperature (about 23°C) for 16 h. The samples were gold-coated and examined via FEI (INSFECTF) SEM device with an accelerating voltage of 30 kV.

The tensile test was performed on an Instron-5567 testing machine at ambient temperature (about 23°C) according to ASTM D 638 and the flexural test was conducted on an AGS-J testing machine according to ASTM D 790. The yield strength (σ_Y) and elongation at break (EB) were obtained from the stress–strain curves of the blends at a crosshead speed of 50 mm min^{-1}. The flexural modulus (E_f) was measured with a loading speed of 2 mm min^{-1}. At least seven specimens were tested and the average values were reported.

Notched I_{zod} impact strength (σ_I) was obtained by using a UJ-40 impact testing machine, according to ASTM D 256. All the specimens were tested at ambient temperature (about 23°C). At least five specimens were tested and the average values were used here.

RESULTS AND DISCUSSION

Figure 1 shows the crystallization and melting curves of the PA 6/iPP blends with different contents of MWCNTs-supported calcium pimelate. The crystallization temperature (T_c) of PA6 and iPP used in this work is 226 and 121°C, respectively. Compared with simple PA 6/iPP blend (AP1), the crystallization peak temperature of iPP ($T_{c\text{-}iPP}$) almost does not change with the introduction of MWCNTs-supported calcium pimelate; on the contrary, the $T_{c\text{-}PA\ 6}$ of nucleated PA 6/iPP blends is much higher than the $T_{c\text{-}PA\ 6}$ of simple PA 6/iPP blend (AP1), indicating that PA 6 is easier to crystallize with certain amount of MWCNTs-supported calcium pimelate which acting as heterogeneous nucleating agent for PA 6. Moreover, the crystallization peaks of PA 6 in P1 samples are much wider than other samples. As pointed out in literature,[36] this peculiar crystallization behavior can be related with fractionalized crystallization, which has relation with the size of dispersing phase and compatibilizer. Because iPP component is still in the melt state during the crystallization process of PA 6, the nucleating effect for PA 6 has to be attributed to MWCNTs-supported calcium pimelate. It can be inferred that during the preparation of nucleated PA 6/iPP blends, a part of

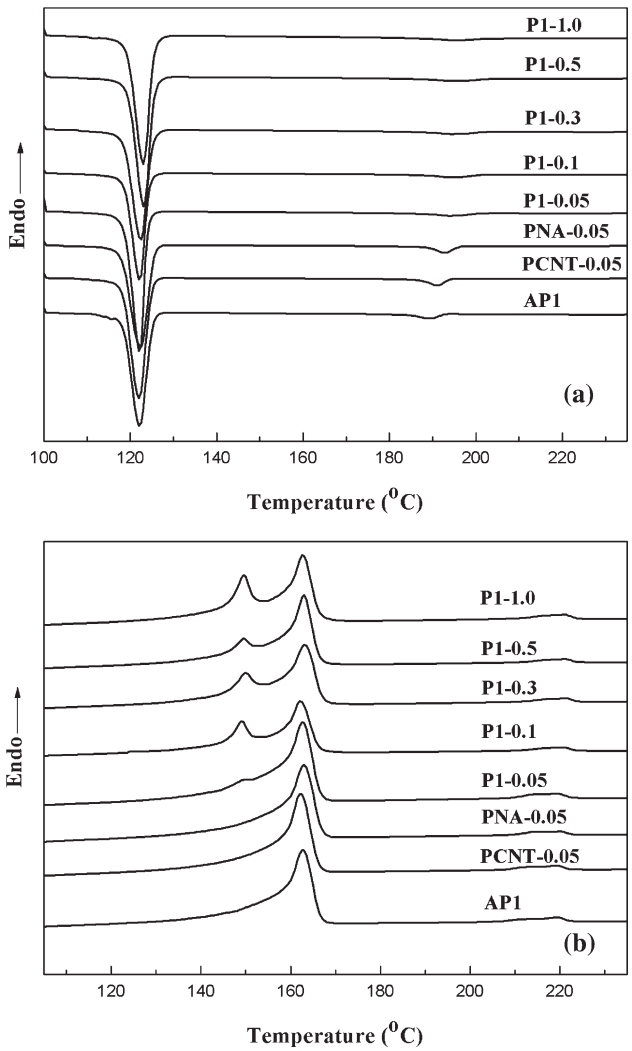

Figure 1 Crystallization (a) and melting (b) curves of the PA 6/iPP blends with 0.05 wt % calcium pimelate, 0.05 wt % MWCNT and different contents of MWCNTs-supported calcium pimelate.

MWCNTs-supported calcium pimelate migrate to the interface of PA 6/iPP blends or into the PA 6 phase because of the polarity attraction or chemical interaction between amino and the remaining carboxyl groups which come from the incomplete reaction of calcium pimelate and MWCNTs. Therefore, in the crystallization process, the crystallization of PA 6 is enhanced at higher T_c in the iPP melt.

Competition between the α nucleating effect of PA 6 and β nucleating effect of MWCNTs-supported calcium pimelate for iPP are clearly observed in the melting curves shown in Figure 1(b). Only one melting peak for iPP in AP1 was observed, which is the melting peak of α-phase of iPP due to the highly efficient α-nucleating effect of PA 6 for iPP. Even when 0.05 wt % calcium pimelate, a highly selective β nucleating agent for iPP, was incorporated into the blend, as shown by the curve labeled as PNA-0.05, there is still only one melting peak of α-phase of iPP, showing no traces of β-phase for iPP. This indicates that at this concentration of calcium pimelate, the α-nucleating effect of PA 6 for iPP surpasses the β nucleating effect of calcium pimelate. However, when 0.05 wt % MWCNTs-supported calcium pimelate was introduced (P1-0.05), a small shoulder peak for iPP at relatively low temperature, the melting peak for β-phase of iPP, around 150°C, is present. Hereafter, the fusion enthalpy of both the β-phase and the α-phase for iPP is increasing with increased content of MWCNTs-supported calcium pimelate, as shown in Table I. The results show that in PA 6/iPP blend, calcium pimelate or MWCNTs both exhibit limited β nucleating effect for iPP component, while the combination of calcium pimelate and MWCNTs by means of chemical supporting shows great capability of inducing the formation of β-iPP crystrals, which even surpass the strong α-nucleating effect of PA 6 for iPP.

In DSC analysis, after the first heating which aims to erase thermal history, PA 6 can induce more iPP to form α-phase during the following crystallization process. Moreover, this melting process is helpful for the β → α transition and some β crystals can recrystallize into α-phase,[2] so the relative crystallinity of β-iPP from DSC results is not convincible. To consolidate the results of DSC, XRD characterization were performed under room temperature and the content β-phase (X_β) were also calculated and listed in Table I. From Figure 2, it is clearly seen that the intensity of β-peak at $2\theta = 16.1°$ and the value of X_β increase with increasing content of MWCNTs-supported calcium pimelate, consistent with the DSC results.

The morphologies of the PA 6/iPP blends are shown in Figure 3. The cryogenic fracture

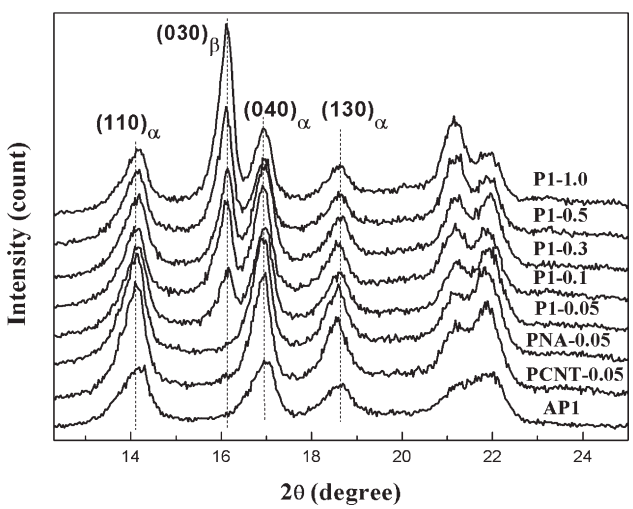

Figure 2 XRD patterns of PA 6/iPP blends with 0.05 wt % calcium pimelate, 0.05 wt % MWCNT and different contents of MWCNTs-supported calcium pimelate.

TABLE I
DSC Data of iPP and PA 6 in PA 6/iPP Blends with 0.05 wt % Calcium Pimelate, 0.05 wt % MWCNT and Different Contents of MWCNTs-Supported Calcium Pimelate

			$T_{m\text{-iPP}}$ (°C)		$\Delta H_{m\text{-iPP}}$ (J gΔ^{-1})		
Samples	$T_{c\text{-PA6}}$ (°C)	$T_{c\text{-iPP}}$ (°C)	β	α	β	α	K_β (%)
AP1	189.3	122.1	–	162.7	–	86.0	–
PNA-0.05	191.1	122.0	–	162.2	–	88.3	–
PCNT-0.05	193.0	122.5	–	162.9	–	90.8	–
P1-0.05	193.8	122.0	151.8	162.7	–	–	14.1
P1-0.1	194.4	122.4	150.8	162.3	52.6	30.6	26.3
P1-0.3	194.3	122.4	152.2	162.9	54.8	32.7	27.6
P1-0.5	194.4	122.7	152.6	162.6	55.9	33.3	42.5
P1-1.0	194.5	123.3	150.3	162.4	57.1	34.0	53.1

Note: the ΔH_m of β-iPP in P1-0.05 blend was too small to be evaluated via the peak fitting software, so it is not listed in Table I.

morphology with and without MWCNTs-supported calcium pimelate are distinctly different. After chemical etching of PA 6 and the amorphous region of iPP matrix, holes are left by PA 6 particles. In addition, it can be seen clearly that iPP crystallizes epitaxially around these holes which shows positive effect in reinforcing the interfacial interaction of PA 6 and iPP components.

Spherulites of α-phase dominate in the blend AP1. As is known, α-iPP is organized in a crosshatched structure and the development of extended plastic damage will not be disturbed by the physical network created by crosshatched crystallites,[37,38] which is visually evidenced by the distinct boundaries of α-crystals which makes the gliding of crystal lamella difficult. Moreover, smooth fracture surface indicates the brittle fracture behavior of the blend AP1.

When MWCNTs-supported calcium pimelate is introduced into PA 6/iPP blends, visible β crystals of iPP emerge. β crystal of iPP exhibits a sheaf-like structure of radial lamellae growing in bundles from a central nucleus without any epitaxial growth of

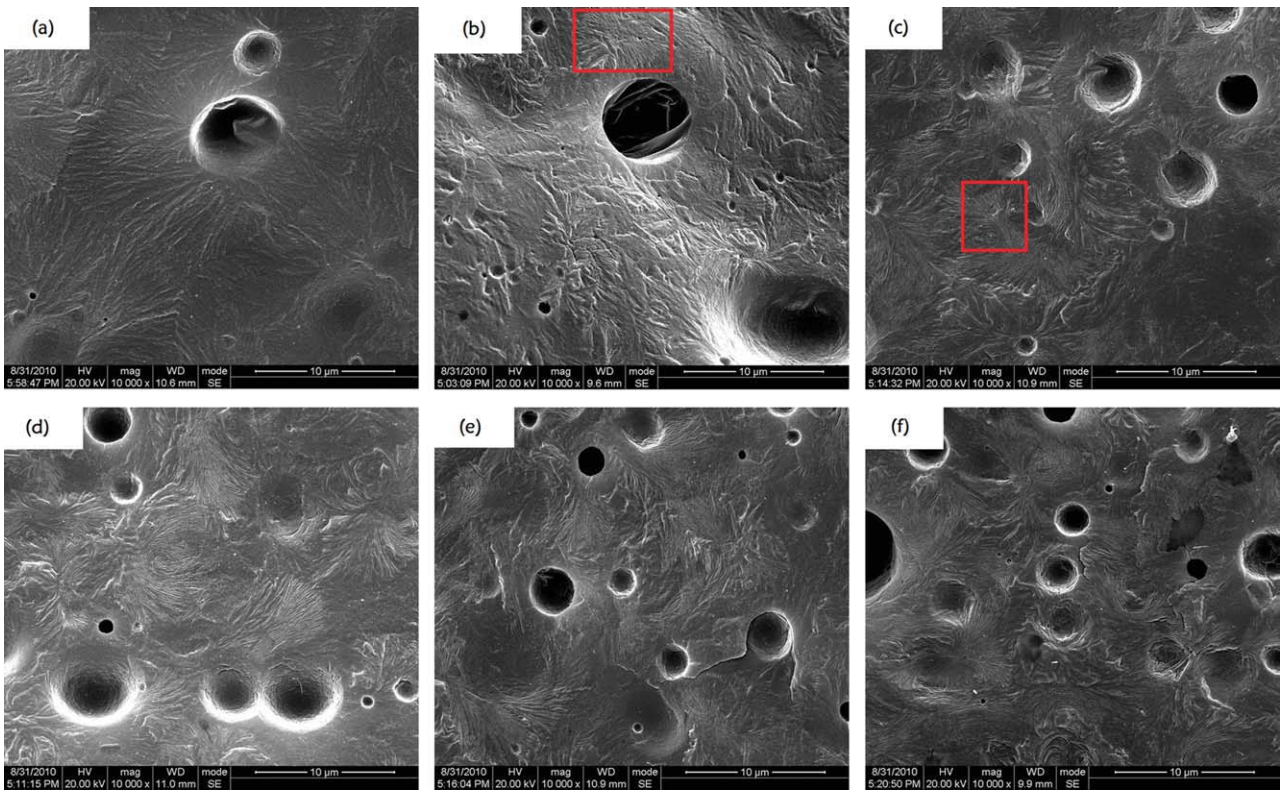

Figure 3 SEM photos of iPP/PA6 blends with different MWCNTs-supported calcium pimelate contents. (a) AP1, (b) P1-0.05, (c) P1-0.1, (d) P1-0.3, (e) P1-0.5, (f) P1-1.0. [Color figure can be viewed in the online issue, which is available at wileyonlinelibrary.com.]

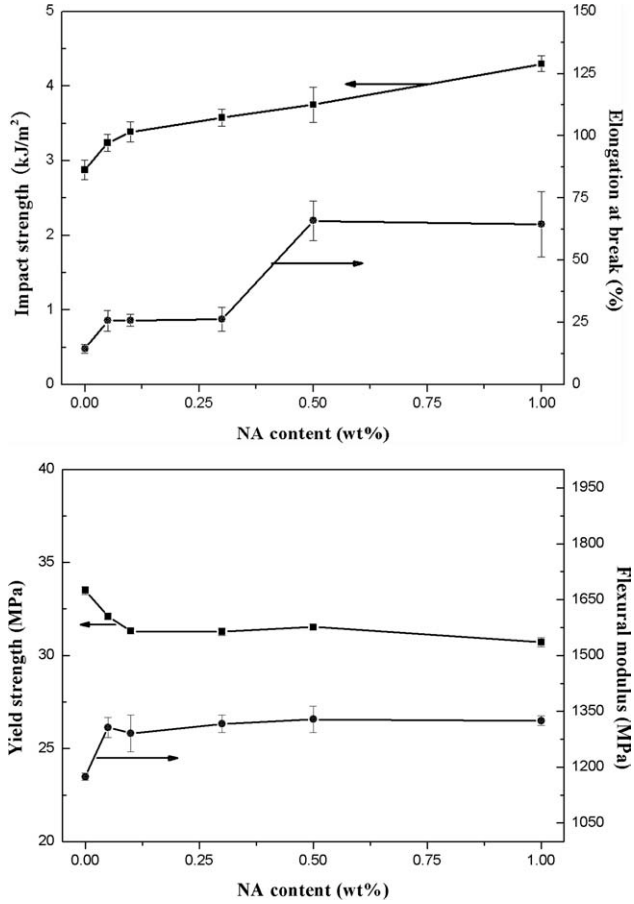

Figure 4 Mechanical properties of iPP/PA6 blends with different contents of MWCNTs-supported calcium pimelate.

tangential lamellae, as shown in Figure 3(b–f), and the lamellae of β crystal of iPP is parallel to each other and orientate perpendicular to carbon nanotubes axis which is located in the middle, as can be seen in the box of P1-0.05 and P1-0.1. When the content of MWCNTs-supported calcium pimelate reaches 0.1 wt %, the lamellae bundles of β crystals largely appears, which consists of edge-on lamellae. In further growth, the lamellae leave the plane of hexagonite due to the branches that cause splaying of their parallel arrangement, and "human face" like arrangement of β crystals,[2] emerges.

In Figure 4, the impact strength and elongation at break are shown to increase with increasing content of MWCNTs-supported calcium pimelate, compared with those of the blend AP1. This phenomenon is consistent with the peculiar characteristic of β-phase of iPP. Superior ductile properties of β-phase has been attributed to: (a) the β to α phase transition induced by mechanical force, accompanying with the densification of the crystal transformation, which will result in fine cavities and absorb more energy, (b) superior mechanical damping of β-phase, and (c) the peculiar crystalline structure of β-phase.[2] As discussed above, the plastic deformation of the β-phase with a sheaf-like structure will happen since the deformation of the amorphous chains (and therefore the lamella separation process) is facilitated in the early stages of a dilatational deformation for the β-phase due to that the absence of "interlocking" structure blocks their mobility, which allows an efficient stress transfer.[37,38]

The impact strength of PA 6/iPP blends with MWCNTs-supported calcium pimelate is enhanced considerably, compared with AP1, which suggests that the MWCNTs-supported calcium pimelate can effectively improve the toughness of PA 6/iPP blends. Moreover, the ductile characteristics, elongation at break, is also improved to some extent, especially when the content of MWCNTs-supported calcium pimelate reaches 0.5 wt % and the samples under tensile test experiences necking process. The reasons for the improved ductility can be explained from two standpoints. On one hand, MWCNTs used here has been functionalized and have hydroxyl groups on the wall, and in the melting process, the remaining hydroxyl groups that did not reacted with calcium pimelate are prone to migrate to the interface of PA 6/iPP blends or into PA 6 phase owning to the interaction between hydroxyl groups and amide group of PA 6; on the other hand, both MWCNTs and calcium pimelate can nucleate iPP in the vicinity of MWCNTs, and consequently, MWCNTs-supported calcium pimelate can reinforce the interaction of iPP and PA 6 matrix synergically. These mechanical results further confirm the DSC thermal behavior and morphologies revealed by XRD characterization and SEM observations.

It is interesting to find that the flexural modulus is still increasing after the MWCNTs-supported calcium pimelate has been introduced into the blends while the yield strength is dropping with increasing content of MWCNTs-supported calcium pimelate. We suppose the main reason of the improvement of flexural modulus can be attributed to the extraordinarily mechanical characteristics of MWCNTs. While the yield strength decreases to some extent compared with simple PA 6/iPP blend owing to the presence of β crystals, which was known to have lower strength compared with α phase iPP. However, it should be noted that the lowering down of the tensile strength does not continue with increasing content of MWCNTs-supported calcium pimelate and increasing content of β phase iPP, which might be compensated by the reinforcing ability of MWCNT as revealed by many literatures.

CONCLUSIONS

A seclective β-nucleating agent for iPP, calcium pimelate, was chemically supported onto the surface of

MWCNTs and the MWCNTs-supported calcium pimelate was introduced into PA 6/iPP (10/90 wt) blends. The results revealed the competition of α and β nucleation between PA 6 and MWCNTs-supported β-calcium pimelate for iPP component in the blends and a low content of MWCNTs-supported calcium pimelate (0.05 wt %) can induce the formation of β-phase iPP, superior than MWCNTs or calcium pimelate. The impact toughness, the elongation at break as well as flexural modulus of PA 6/iPP blends with MWCNTs-supported calcium pimelate was improved compared with simple PA 6/iPP blend while the tensile strength was not significantly depressed which brings this newly designed β-nucleating agent a bright prospect for its application in PA 6/iPP blends.

The authors are also heavily indebted to Mr. Zhu Li from Center of Analysis and Test of Sichuan University for careful SEM observation.

References

1. Lotz, B.; Wittmann, J. C.; Lovinger, A. J Polymer 1996, 37, 4979.
2. Varga, J. J Macromol Sci B 2002, 41, 1121.
3. Crissman, J. M. J Polym Sci A-2 Polym Phys 1969, 7, 389.
4. Padden, F. J.; Keith, H. D. J Appl Polym Sci 1959, 30, 1479.
5. Fujiwara, Y. Colloid Polym Sci 1975, 253, 273.
6. Somani, R. H.; Hsiao, R. S.; Nogales, A.; Srinivas, S.; Tsou, A. H.; Sics, I.; Balta-Calleja, F. J.; Ezquerra, T. A. Macromolecules 2000, 33, 9385.
7. Zhao, S. C.; Cai, Z.; Xin, Z. Polymer 2008, 49, 2745.
8. Zhang, Z. S.; Wang, C. G.; Yang, Z. G.; Chen, C. Y.; Mai, K. C. Polymer 2008, 49, 5137.
9. Varga, J.; Menyhárd, A. Macromolecules 2007, 40, 2422.
10. Bai, H. W.; Wang, Y.; Zhang, Q.; Liu, L. J Appl Polym Sci 2009, 111, 1624.
11. Leugering, H. J Makromol Chem 1967, 109, 204.
12. Li, J. X.; Cheung, W. L.; Jia, D. Polymer 1999, 40, 1219.
13. Bai, H. W.; Wang, Y.; Zhang, Z. J.; Han, L.; Li, Y. L.; Liu, L.; Zhou, Z. W.; Men, Y. F. Macromolecules 2009, 42, 6647.
14. Zhang, R. H.; Shi, D.; Tjong, S. C.; Li, R. K. Y. J Polym Sci Polym Phys 2007, 45, 2674.
15. Shu, Y.; Ye, L.; Zhao, X. W. Polym Plast Technol Eng 2006, 45, 963.
16. Li, J. F.; Yang, R.; Yu, J. Adv Mater Process 2007,26–28,1075.
17. Xiao, W. C.; Wu, P. Y.; Feng, J. C.; Yao, R. Y. J Appl Polym Sci 2009, 111, 1076.
18. Xiao, W. C.; Wu, P. Y.; Feng, J. C. J Appl Polym Sci 2008, 108, 3370.
19. Phillips, A.; Zhu, P. W.; Edward, G. Polymer 2010, 51, 1599.
20. Wei, Z. Y.; Zhang, W. X.; Chen, G. Y.; Liang, J. C.; Yang, S.; Wang, P.; Liu, L. A. J Therm Anal Calorim 2010, 102, 775.
21. Agrawal, P.; Oliveira, S. I.; Araújo, E. M.; Melo, T. J. A. J Mater Sci 2007, 42, 5007.
22. Shi, D.; Chen, H. B.; Li, R. K. Y. J Mater Sci 2007, 42, 9459.
23. Kusomono, Z. A.; Ishak, M.; Chow, W. S.; Takeichi, T. Eur Polym Mater 2008, 44, 1023.
24. Kusmono; Ishak, Z. A. M.; Chow, W. S.; Takeichi, T.; Rochmadi. Compos Part A-Appl S 2008, 39, 1802. http://www.sciencedirect.com/science/article/pii/S1359835X08002285.
25. Macro, C.; Ellis, G.; Gómez, M. A.; Fatou, J. G.; Arronas, J. M.; Campoy, I.; Fontecha, A. J Appl Polym Sci 1997, 65, 2665.
26. Othman, N.; Hassan, A.; Rahmat, A. R.; Wahit, M. U. Polym Polym Compos 2007, 15, 217.
27. Varga, J. J Therm Anal 1989, 35, 1891.
28. Yang, Z. G.; Zhang, Z. S.; Tao, Y. J.; Mai, K. C. J Appl Polym Sci 2009, 112, 1.
29. Yang, Z. G.; Chen, C. Y.; Liang, D. W.; Zhang, Z. S.; Mai, K. C. Polym Int 2009, 58, 1366.
30. Esawi, A. M. K.; Salem, H. G.; Hussein, H. M.; Ramadan, A. R. Polym Compos 2010, 31, 772.
31. Wang, S. W.; Yang, W.; Bao, R. Y.; Xie, B. H.; Yang, M. B. Colloid Polym Sci 2010, 288, 681.
32. Zhang, S. J.; Lin, W.; Zhu, L. B.; Wong, C. P.; Bucknall, D. G. Macromol Chem Phys 2010, 211, 1348.
33. Li, J. X.; Cheung, W. L. J Vin Addit Technol 1997, 3, 151.
34. Jones, A. T.; Aizlewood, J. M.; Beckett, D. R. Angew Makromol Chem 1964, 75, 134.
35. Olley, R. H.; Bassett, D. C. Polymer 1982, 23, 1707.
36. Mbarek, S.; Jaziri, M.; Chalamet, Y.; Elleuch, B.; Carrot, C. Int J Mater Form 2009, 2, 15.
37. Tjong, S. C.; Shen, J. S.; Li, R. K. Y. Polym Eng Sci 1996, 36, 100.
38. Aboulfaraj, M.; G' Sell, C.; Ulrich, B.; Dahoun, A. Polymer 1995, 36, 731.